Boundary Layer Flow over a Bump: Benchmark Experiments for CFD Validation

Version 6: 20 April 2020

Test Case Coordinators

This experiment is being coordinated among three groups, as follows:

Virginia Tech, US:	Sintef Ocean, Norway:	University of Toronto Institute for Aerospace Studies, Canada:
Todd Lowe and William Devenport E-mail: kelowe@vt.edu ; devenport@vt.edu Phone: +540 231 7650 Student Contacts: Julie Duetsch-Patel and Aldo Gargiulo Virginia Tech, US E-mail: jduetsch@vt.edu ; galdo@vt.edu	Luca Savio E-mail: Luca.Savio@sintef.no Phone: +47 930 02 036 Student Contacts: Lars Engan and Yngve Lilleeng Jenssen NTNU, Norway E-mail: larsenga@stud.ntnu.no; yngvelj@stud.ntnu.no	Philippe Lavoie E-mail: lavoie@utias.utoronto.ca Phone: +416 667 7716 Student Contact: Daniel MacGregor and Blago Hristovski UofT, Canada E-mail: TBD; blago.hristovski@mail.utoronto.ca

Overview

A study of low Mach number, high Reynolds number flow of a plane turbulent boundary layer over a wall-mounted bump, the BEVERLI (**BE***nchmark* **V***alidation* **E***xperiment* for **R***ANS* and **L***ES* **I***nvestigations*) hill, is underway. The goal is to produce detailed experimental data sets of smooth wall flows subjected to three-dimensional pressure gradients that lead to various levels of separation. This test case is being run in facilities at three different institutes, providing an opportunity to explore a wide range of scales and facilities boundary conditions.

Virginia Tech Experiment

Introduction

This experiment has been designed and planned to meet the most exacting requirements of CFD validation as per Oberkampf and Smith [1]. To attain this goal, an intensive research program, collaborative with NASA Langley Research Center, is underway that brings together experts in experiments, computations, CFD validation and turbulence modeling. This effort involves detailed measurements and calculations needed for experimental configuration design, detailed uncertainty quantification, and extensive documentation of the flow boundary conditions and boundary condition sensitivities. Initial results of reduced-scale experiments have been published by Gargiulo *et al.* [2] and Lowe *et. al* [3], which will provide further general understanding of the flow cases.

Test Case Description

This test case is set up in the Virginia Tech (VT) Stability Wind Tunnel. The test section is nominally a rectangular cuboid $1.85\ m$ by $1.85\ m$ in cross section and $7.32\ m$ long. The boundary layer under test is generated on the port-side wall of the test section, appearing at the bottom left of Figure 1. The coordinate system used is illustrated in Figure 1. Coordinate x is measured from test section entrance, defined as the end of the contraction profile (where the cross-section becomes $1.85\ m \times 1.85\ m$, identifiable as the joint between the contraction and the first panel of the test section), in the downstream direction, y is measured from and perpendicular to the port-side test wall, and z completes a right-handed system. In the 2D view of the schematic shown in Figure 1, the origin is at the port-side boundary layer wall, at an equal distance of 0.925 *m* from the floor and ceiling.

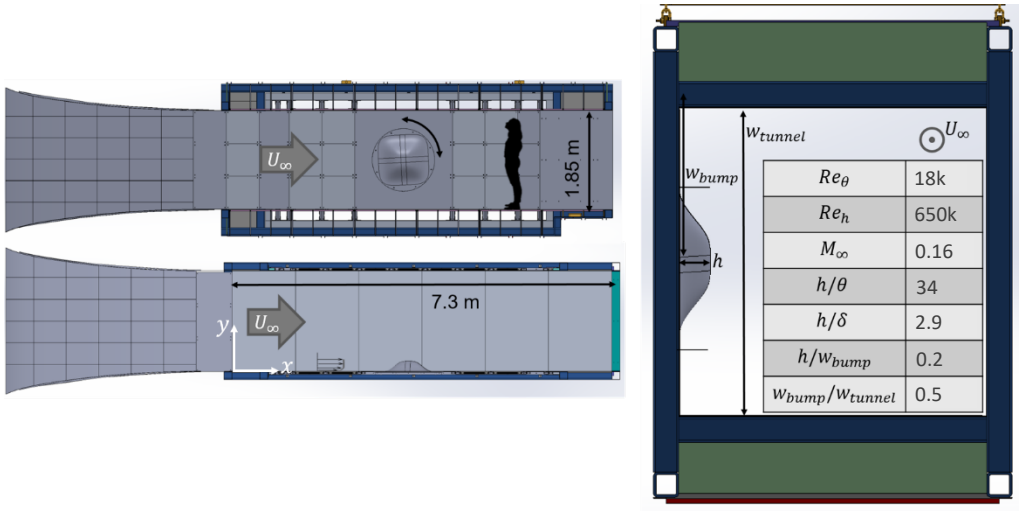

Figure 1: Schematic of the test section configuration with bump installed. Top left: test section side view; Bottom left: contraction and test section top view; Right: Test section cross section with flow coming out of the page. The inset table provides the target-scale flow parameters at the maximum Reynolds numbers planned.

The boundary layer is tripped in the wind tunnel contraction upstream of the test section entrance at $x = -4.43\ m$. At this point the contraction cross-sectional area is 1.66 times that of the test section. The trip has a 27.6-degree zig-zag planform pattern periodic on $10\ mm$ with a total height of $3.18\ mm$ and a total streamwise width of $20.39\ mm$. The boundary layer is has been measured along the span of the test wall,

with more detailed spanwise measurements planned for 2020. It has a thickness of around $45\ mm$ at $x = 1.2\ m$ and $78\ mm$ at $x = 5.3\ m$ at bump height-based Reynolds number of approximately 715,000. The as-tested geometry of the test section and contraction will be available in the form of point clouds extracted from laser scans. The laser scanner used has a resolution of $1.2\ mm$ and a ranging error of $\pm\ 1\ mm$ at distances up to $25\ m$ from the target. The ranging error is defined as the maximum error in the distance measured by the scanner from its origin point to a point on a planar target. Some components of these data are also available as CAD files.

The bump geometry has been reported in past work [2,3], excerpts of which are reproduced here. The fully analytic bump geometry (see Figure 2) is generated by requiring continuous curvature in all three dimensions, while allowing for flat sections on the four sloping sides and a flat top. A fifth-order polynomial provides enough parameters to meet these conditions for generating the curved sections fairing to the floor and to the flat top. The four sloping sides yield continuous curvature by creating corners described by a superellipse with exponent equal to 4 (see Figure 3).

The bump geometry further exhibits rotational symmetry every 90 degrees in yaw, which allows for different orientations of the bump with respect to the incoming flow of the VT Stability Wind Tunnel at various angles in the range $[0, \pi/2]$ rad. This enables the generation of the different target flow separation regimes.

The bump scaling is based on the tunnel geometry and tunnel boundary layer scales. Specifically, the boundary layer thickness $\delta \cong 63\ mm$ at the center of the test section, the flow conditions are set by Reynolds number, where the maximum height-based Reynolds number, Re_h, is 650,000,corresponding to a nominal free-stream velocity of $U_\infty = 55\ m/s$ and Mach number of $M_\infty = 0.16$ for our scales. Furthermore, a bump width to boundary layer thickness ratio $w/\delta = 14$ and a bump height to boundary layer thickness ratio $h/\delta \cong 3$ are selected as desired values for the bump geometry design. The choice of the latter features was informed by already existing studies of bump flow conducted by other research groups and were thought to place the study in the proper parameter space for achieving three separation regimes (attached flow, incipient separation, and massive smooth-body turbulent separation) on varying parts of the bump or at varying orientations.

Note, the initial design of the bump geometry is performed utilizing Imperial units and reported as such throughout this description of the bump geometry to avoid the introduction of round-off inaccuracies from converting bump geometry parameters to SI units. Reporting these parameters exactly as designed, using Imperial units, will assure a higher accuracy when attempting to recreate this geometry from the description of this document.

The 2D centerline cross-section of the full 3D bump geometry is represented by the connection of two mirrored 5th degree polynomial profiles $P_5(x)$ with a flat top. Considering the coordinate system in Figure 2 and Figure 3, the polynomial is first fitted on the positive x-axis imposing the 6 polynomial constraints depicted in Table 1. Note, these constraints impose a zero-slope and zero-curvature condition at the boundaries of the polynomial. The generated polynomial profile face is mirrored about the $x = 0$ axis to form the opposite face of the bump on the negative x-axis. A flat top of length $s = 3.68\ in = 0.093472\ m$ connects the two polynomial faces to form the complete 2D bump profile shown in Figure 2, where the polynomial faces are depicted by a blue curve and the flat top by a red curve.

The exact corresponding coefficients of the 5th degree polynomial are summarized in Table 2. Note, these coefficients are based on Imperial units.

Table 1: Constraints of 5th Degree Polynomial

Function	$P_5(s/2) = h$	$P_5(w/2) = 0$
1st Derivative	$P_5'(s/2) = 0$	$P_5'(w/2) = 0$
2nd Derivative	$P_5''(s/2) = 0$	$P_5''(w/2) = 0$

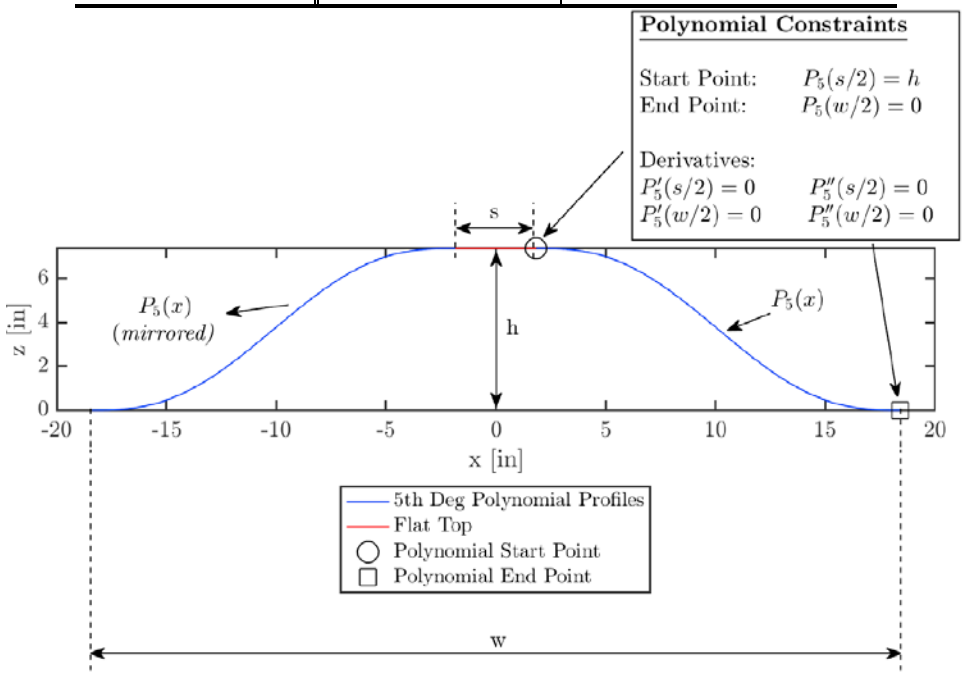

Figure 2: 2D Bump with 5th Degree Polynomial Faces

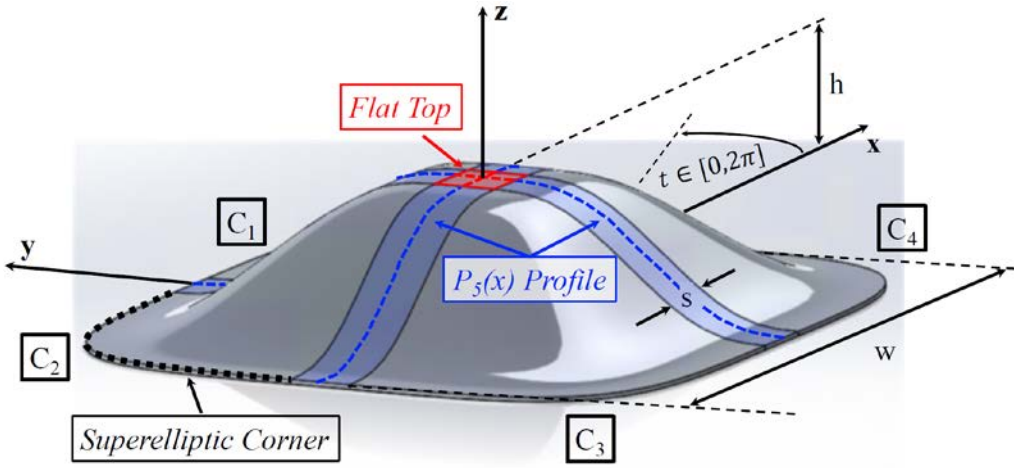

Figure 3: Main Features of 3D Bump Design

Table 2: $P_5(x)$ Coefficients in Imperial Units (inches^{1-m}, where m is the polynomial coefficient subscript).

$\boldsymbol{z(x) = P_5(x) = a_5x^5 + a_4x^4 + a_3x^3 + a_2x^2 + a_1x + a_0}$ $\boldsymbol{x \in \left[\frac{s}{2}, \frac{w}{2}\right]}$	
$\boldsymbol{a_5}$	$-35.4590750202868 \times 10^{-6}$
$\boldsymbol{a_4}$	$1.79422919602651 \times 10^{-3}$
$\boldsymbol{a_3}$	$-28.2118074313405 \times 10^{-3}$
$\boldsymbol{a_2}$	$121.490847321347 \times 10^{-3}$
$\boldsymbol{a_1}$	$-203.221053701163 \times 10^{-3}$
$\boldsymbol{a_0}$	7.47853477620281

To generate the complete 3D bump geometry, the 2D profile is first extruded spanwise a length of $s/2$ both along the positive and the negative y-axis. This creates a straight cylindrical body of thickness s, which is represented in Figure 3 by red and blue shaded surfaces. The colored dashed line at the center of the shaded surfaces, hereby, symbolizes the 2D bump profile through the centerline of the 3D geometry. The cylindrical section is rotated by 90 degrees in the mathematical positive sense about the z-axis to generate the aforementioned 90 degrees rotational symmetry. This rotation also generates a squared flat top, which is highlighted by a red solid line in Figure 3. This flat top further facilitates optical flow measurements on the surface of the bump such as Particle Image Velocimetry (PIV). The corners of the bump are completed by rotating the $P_5(x)$ polynomial face about each corner of the flat top, constraining the rotation by a superelliptic curve at the bump base. In Figure 3, the corners are labeled as $C_i = 1, 2, 3, 4$.

Given the above selected parameters and taking into account limitations imposed by the manufacturing of the physical bump model, a bump width of $w = 36.8\,in = 0.93472\,m$ and a bump height of $h = 7.36\,in = 0.186944\,m$ are selected. Images of the as-manufactured bump in the VT Stability Wind Tunnel in February 2020 are shown in Figure 4**Error! Reference source not found.**.

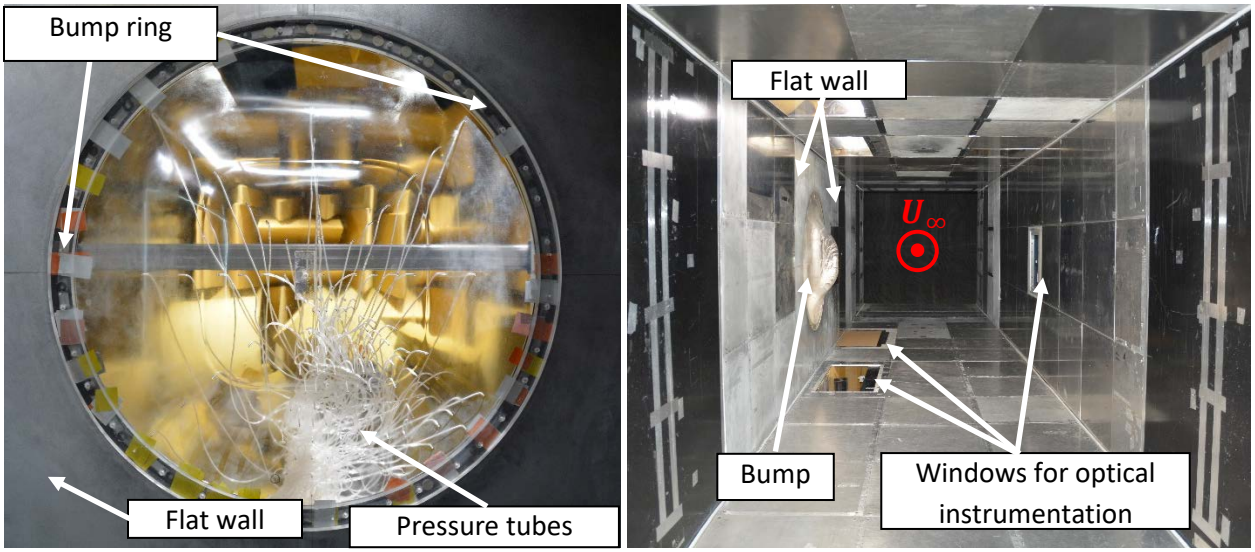

Figure 4: Left: A plan view image of the transparent bump model used in February 2020 experiments; Right: VT Stability Wind Tunnel test section with the bump mounted on the port wall in February 2020.

Some basic flow features in the test case

The test case is intended to include key physics features of pressure-driven, three-dimensional boundary layers with and without separated flow regions. To give a sense of the flow features that will be present in the test case, some observations made during the design of the experiment are provided to follow.

During the initial design of the bump geometry, panel method calculations were conducted to obtain the ideal flow over the bump. Contour plots of the pressure coefficient $C_p$computed for two yaw angles differing by 45 degrees are shown in Figure 5. These calculations should only be considered notionally representative for the windward sides of the bump, while the leeward side results should be ignored due to likely separation. The results from the two yaw angles indicate that substantial variation in the pressure gradient structure is possible by simple rotation of the same geometry. Other features to note are the three-dimensional stagnation region near the base of the windward side of the 0-degree yaw case, and

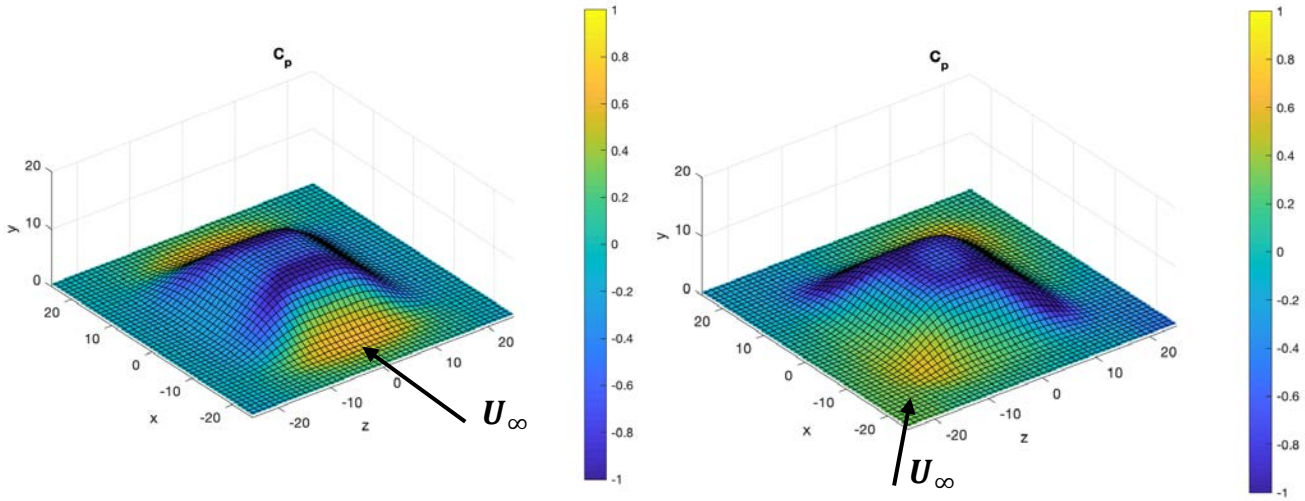

Figure 5: Panel method calculations for the full-scale flow over the bump. (L) At the default yaw angle, 0 deg. (R) At a secondary yaw angle, 45 deg.

the multi-peaked nature of the pressure coefficient at the bump top owing to the flat region.

For qualitative understanding of the flow features, a reduced Reynolds number experiment ($Re_h = 325k$ was conducted in the VT Stability Wind Tunnel using oil flow visualization and wall static pressure instrumentation. As shown in Figure 6, region A, the bump exhibits a high shear region near the top, as flow accelerates around the curvature. Interestingly at lower Reynolds numbers, this region was observed to separate, presumably due to relaminarization. Future studies of the lower Reynolds number regime could serve as cases for relaminarization physics and modeling but are beyond the scope of this activity. In Figure 6 region B, the leeside separation region is shown, revealing a characteristic cardioid pattern of three-dimensional, smooth wall separation.

As seen in Figure 7, the pressure distribution across the centerline of the bump is characterized by a "double hump" due to the flat surface along the top of the bump. The pressure distributions responds sensitively to both the Reynolds number and the boundary layer thickness δ, allowing for more flow parameters to be manipulated to change the flow over the bump as desired.

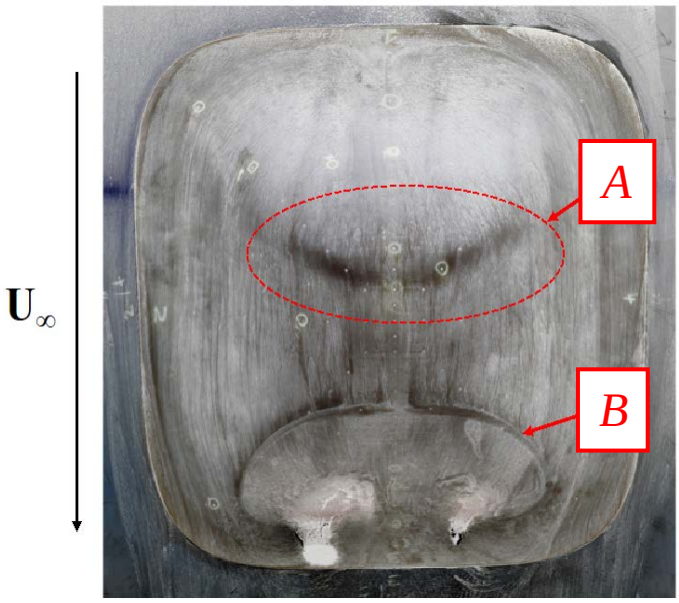

Figure 6: Surface oil flow visualization for a reduced Reynolds number experiment. (A) high shear region, (B) separation bubble

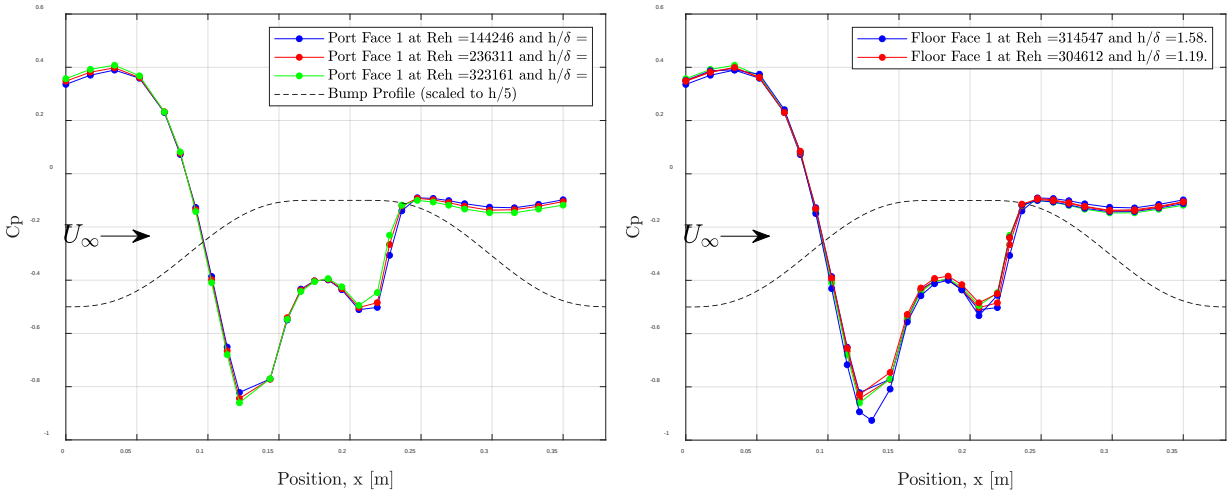

Figure 7: Bump centerline pressure distributions from reduced Reynolds number experiment. (L) Pressure distribution varying with Reynolds number. (R) Pressure distribution varying with boundary layer thickness.

Overall Test Section Aerodynamic Conditions

Experiments will be conducted at three height-based Reynolds numbers equal to 325,000, 487,500, and 650,000. These correspond to flow velocities, U_∞, in the test section of nominally 30 m/s, 40 m/s, and 55 m/s, respectively; but since the test condition is set by Reynolds number, the actual velocity varies ± 5 m/s based on daily conditions. Tunnel free stream velocity is measured using ports located in the settling chamber and contraction. Measurements are transformed using calibration factors as a function

of the true free stream pressure and velocity determined by Pitot-static probe measurements at $X = 3.31\ m$ (approximately the bump location) in the empty test section. The equations and calibration factors are available. Ambient pressure is sensed in the "control room" area of the Stability Tunnel, on the outside wall of the contraction, and is nominally equal to the empty test section static pressure. Flow temperature is sensed using an Omega type 44004 thermistor on the boundary layer wall at $x = 7.5\ m$, $z = 0.7\ m$ with an uncertainty of $\pm 0.2\ K$.

The mean flow velocity and static pressure are closely uniform ($C_p \approx \pm 0.003$) over the empty test section inflow plane, except for the wall boundary layers; and lateral and spanwise velocity components are close to zero. Actual inflow uniformity measurements, in the absence of the bump, are available for about 30% of the cross-sectional $y - z$ plane at $x = 1.2\ m$ and will be available for this entire plane. This data set also includes measurements of the nominally identical boundary layers on the other 3 test section walls. Outflow uniformity measurements for the empty test section are available for 70% of the cross-sectional $y - z$ plane at $x = 6\ m$, which shows a uniformity on the order $C_p \approx \pm 0.01$.

Free stream turbulence intensity measurements at the empty test section center point, based on historical data are 0.021% at $30\ m/s$ and 0.031% at $57\ m/s$. Velocity spectra from measurements used to determine these turbulence levels are also available. Additional empty test section turbulence and uniformity measurements are planned for 2020.

While exact dimensional aerodynamic conditions depend on ambient atmospheric conditions, typical conditions that should be used for flow calculations are:

- Static density $1.156\ kg/m^3$
- Static sound speed $340\ m/s$
- Static Temperature $284\ K$
- Atmospheric Pressure $94\ kPa$
- Kinematic Viscosity $1.53 \times 10^{-5}\ m^2/s^2$
- Free stream turbulence intensity 0.03%

Overall Form of the Boundary Layer

Preliminary measurements giving the overall scale of the boundary layer flow at the inflow with the bump installed are presented in this section. These measurements are presented to give an overall concept of the scale of the flow. Mean velocity measurements of the flow were made for free-stream velocities of approximately $25\ m/s$, $37\ m/s$, and $65\ m/s$ (height-based Reynolds numbers of 325,000, 488,000, and 650,000).

Figure 8 shows a preliminary measurement of the smooth wall boundary layer profile near the inflow at $(x, z) = (1.25, 0)\ m,\ 5.68\ m$ downstream of the trip and approximately $1.4\ m$ upstream of the windward foot of the bump. Further spanwise boundary layer measurements at the inflow will be conducted later in 2020.

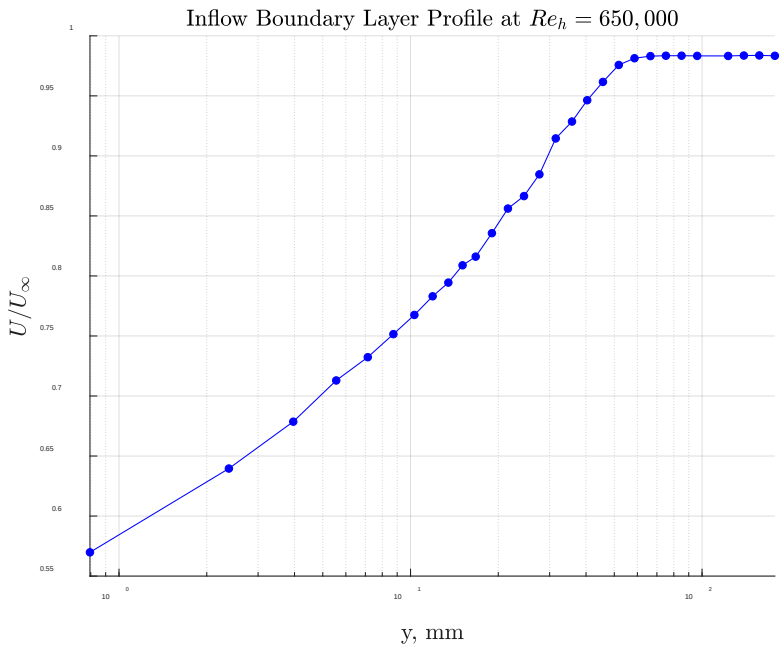

Figure 8: Example Smooth Wall Inflow Boundary Layer Profile

Measurements to be made

a) Ambient pressure and flow temperature
b) Mean pressure measurements are made using the following arrays of 1/16 inch outer diameter (0.0425 inch inner diameter) taps
   i. 64 pressure taps in the contraction distributed each of the 4 walls in arrays consisting of streamwise rows at $\pm$ 100 mm from the centerline and rings at $x = -1.5\ m$ and $x = -5.6\ m$.
   ii. 82 pressure taps on the port and starboard walls between $x = 0.2\ m$ and $5.4\ m$ and $z = -1\ m$ and $1\ m$ with a typical streamwise resolution of $100\ mm$ and spanwise resolution of $600\ mm$
   iii. 132 pressure taps on the bump, concentrated in one octant, with taps placed in symmetric locations in the other seven octants for uncertainty quantification
c) Mean velocity profiles on the port wall at 2 locations ranging from $x = 1.3\ m$ to $1.9\ m$ at $z = 0\ m$ and 1 location at $z = \pm 0.61\ m$ (inflow into the test section). All measurements with be available for the full set of Reynolds numbers.
d) Planar and stereoscopic time-resolved PIV measurements of mean velocity components, turbulence stresses, velocity spectra, space-time correlations and other properties determined from planar instantaneous flow field data, resolved at $12.85\ kHz$. Measurements will be available for $x = 1.3\ m$ at $z = 0\ m$ for the full set of Reynolds numbers. Measurements of the boundary layer development around and over the bump and within the bump wake will also be made

available. Stereo PIV measurements will be analyzed using the method of Volino *et al.* to obtain estimates of wall shear stress [4].

e) Three-velocity component embedded laser Doppler velocimetry (LDV) measurements near the bump surface to complement PIV measurements and provide indirect wall shear stress measurements via fits to sublayer data.

f) Surface pressure fluctuation measurements, including spectra and space time correlations, measured along the cylindrical and flat top sections of the bump, as well as in the wake.

g) Oil film interferometry for direct wall shear stress measurements upstream and over the bump.

Note that measurements a) through b) are repeated with each of the measurements c) through e). These repetitions provide validation of consistent flow conditions, or measurements of the departure there from and can be provided individually if requested.

A diagram indicating expected distribution of detailed flow measurements is shown in Figure 9, where the bump is represented by five contours and the flow direction is from left to right. These locations as currently specified will be adjusted according to findings and constraints from the experiments.

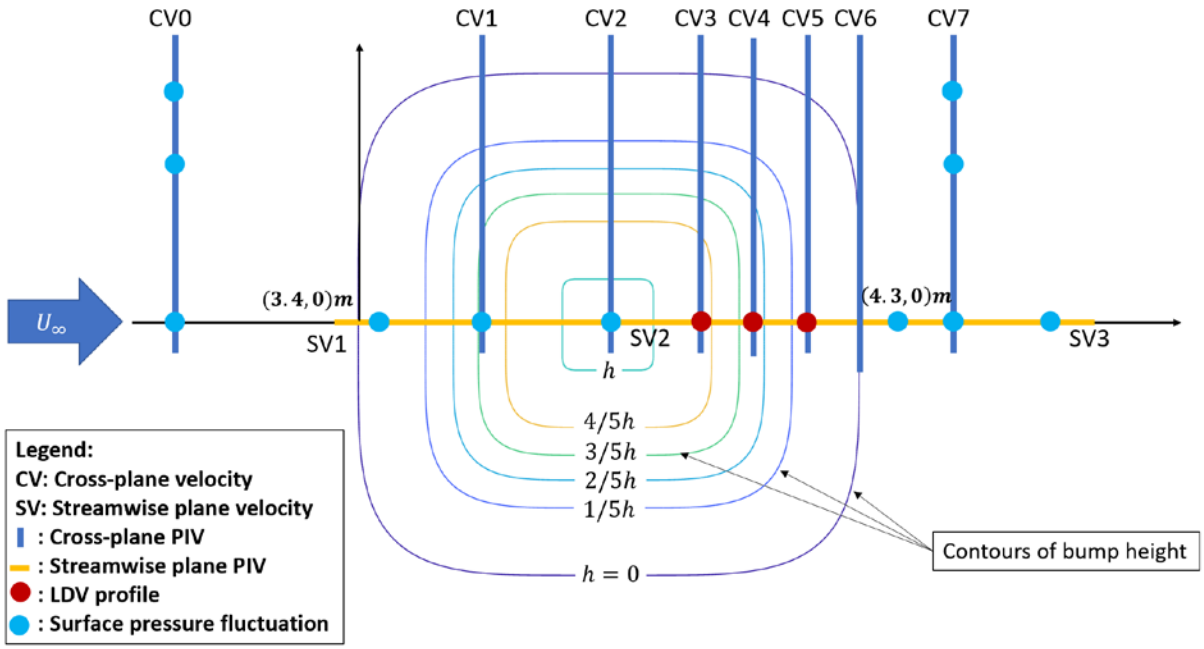

Figure 9: Expected distribution of detailed flow measurements (bump is represented by concentric contours, flow direction is from right to left).

References

[1] Oberkampf, W. L., and Smith, B. L. "Assessment Criteria for Computational Fluid Dynamics Model Validation Experiments." *Journal of Verification, Validation and Uncertainty Quantification*, Vol. 2, 2017. doi:10.1115/1.4037887.

[2] Gargiulo, A., Vishwanathan, V., Fritsch, D. J., Duetsch-Patel, J. E., Szoke, M., Borgoltz, A.,

Devenport, W. J., Roy, C. J., and Lowe, K. T. “Examination of Flow Sensitivities in Turbulence Model Validation Experiments.” *AIAA SciTech 2020 Forum*, Orlando, FL, Jan 6, 2020., AIAA 2020-1583.

[3] Lowe, K. T., Beardsley, C., Borgoltz, A., Devenport, W. J., Duetsch-Patel, J. E., Fritsch, D. J., Gargiulo, A., Roy, C. J., Szoke, M., and Vishwanathan, V. “Status of the NASA/Virginia Tech Benchmark Experiments for CFD Validation.” *AIAA SciTech 2020 Forum*, Orlando, FL, Jan 6, 2020., AIAA 2020-1584.

[4] Volino, R. J., and Schultz, M. P. “Determination of Wall Shear Stress from Mean Velocity and Reynolds Shear Stress Profiles.” *Physical Review Fluids*, Vol. 3, 2018. doi:10.1103/PhysRevFluids.3.034606.

Sintef Ocean Experiment

Covid-19 status:

Please note that due to the restrictions imposed in Norway due to the Covid-19 outbreak, there may be delays in the schedule. At this time, it is still too early to say what they may be, and the project team will keep the group updated.

Introduction

The purpose of this test case is to provide validation data for CFD turbulence modelling in separated regions due to three-dimensional pressure gradients in a turbulent boundary layer flow over a bump. The test case defined by Lowe and Devenport [1] in the Virginia Tech stability wind tunnel is used as a base, but some modifications are made to the experimental setup. The main difference is that the experiments will be done in water rather than in air. Also, instead of mounting the bump on the test section wall it will be mounted on both sides of a smooth flat splitter-plate in the middle of the test section to allow for force measurements. The test case will be divided into two stages; one large scale high Reynolds number experiment in the Cavitation Tunnel of *SINTEF OCEAN* planned for 2021 and a smaller scale low Reynolds number experiment in the *Circulating Water Tunnel* (*CWT*) of *NTNU* which will be conducted this year. This document considers the latter. An important goal of this test case will therefore be to examine flow sensitivities that may disturb the desired flow pattern as described by Gargiulo et al. [2], but also to test the experimental setup before the big scale experiments.

Several experimental techniques will be used to examine the flow around the bump, among these are:

- Stereo PIV to capture mean and instantaneous flow velocities
- LDV point measurements to examine boundary layer in front of and on the bump
- Flow visualization with fluorescein dye to visually observe flow patterns and instabilities
- Force measurements on the bump to observe whether global asymmetries and oscillatory flow phenomena are present with the aim to monitor the stability of the experiments

Test Case Description

The main goal of the test case is to observe and quantify the three flow regimes: attached flow, incipient separation and smooth-body turbulent separation. A three-dimensional bump geometry will be used to achieve this. The curvature of the bump will create the favorable and adverse pressure gradients leading to the three wanted flow regimes. The bump geometry is identical to the Virginia Tech Bump described by Lowe and Devenport [1] but will be uniformly scaled to a height of 60mm. The bump will be placed on both sides of a smooth flat splitter-plate which will be placed in the middle of the test section. The main design dimensions of the bumps and the splitter-plate are presented in Figure 10. The placement of the bump on the plate together with the inflow velocity will determine the bump height to boundary layer thickness ratio which is an important parameter in the experiments.

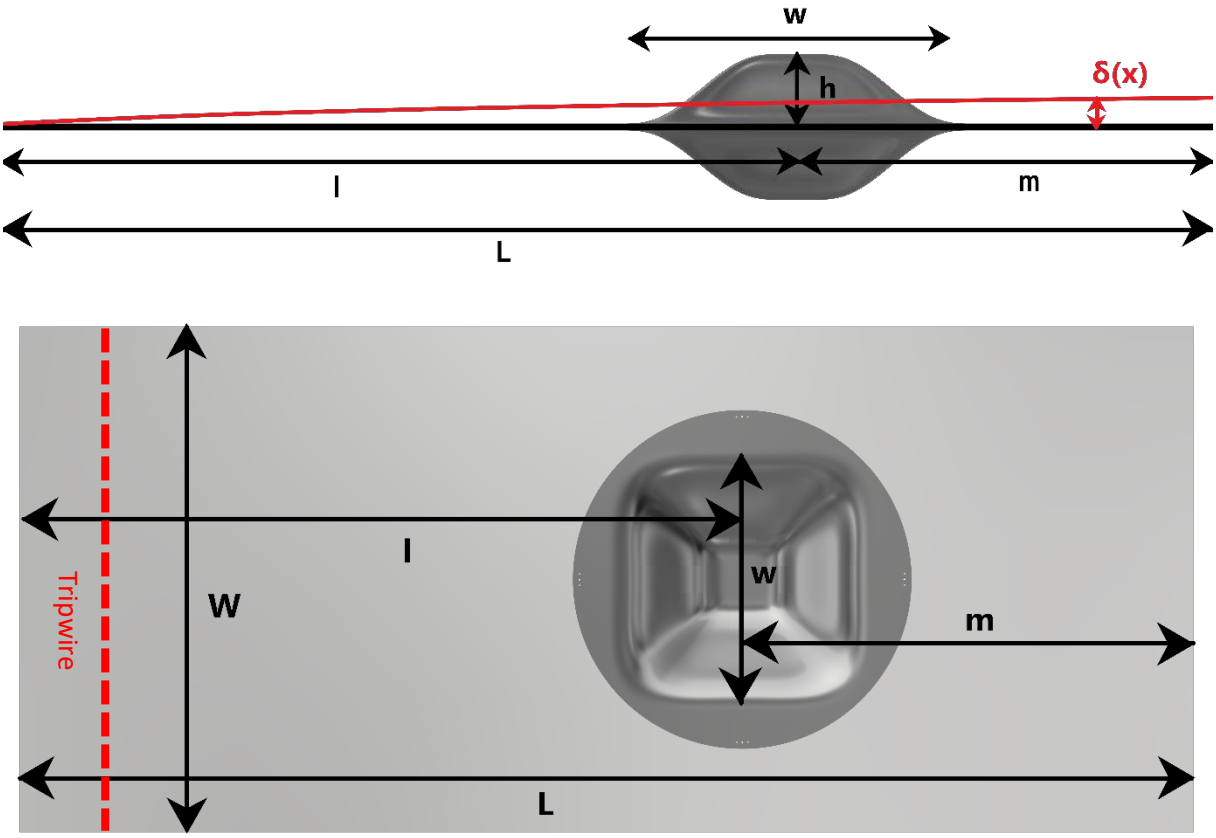

Figure 10: Bump and splitter-plate design dimensions seen from the side and the top. The inflow is coming from the left and the boundary layer will develop over the length l before it comes to the centre of the bump.

Following Lowe and Devenport [1] the bump will be designed to work at h/δ ≅ 3, but the exact value will first be known after the boundary layer on the plate is examined. The boundary layer on the plate will be measured with both PIV and LDV to get detailed information about its thickness at the bump position. Initially, the placement of the bump on the plate is based purely on theoretical calculations; it is placed such that the desired bump height to boundary layer thickness is achieved at 0.9 m/s. At this speed the Reynolds number based on x-position from the tip of the plate, Re_x, is only $7 * 10^5$ which means that the boundary layer has not yet become fully turbulent. Therefore, the boundary layer will be tripped using a tripwire at 10% length from the tip of the plate. The main experimental scales are given in Table 3:

Test section size	0.6m X 0.6m
Model height, h	0.06m
Model width, w	0.3m
Plate length, L	1.3m
Plate width, W	0.56m
Bump placement upstream, l	0.8m
Bump placement downstream, m	0.5m
Max U_∞	0.9m/s
Max Re_h	53 900
Min U_∞	0.03m/s
Min Re_h	1800

h/δ	3
w/δ	15

Table 3: Main experimental scales for the CWT experiments

The experiments will be performed in the CWT facility at NTNU. This is a smaller circulating water tunnel with a quadratic cross section of 0.6 m by 0.6 m which is 2.29 m long (the observable part). The test section can be run with a roof or with a free surface. The water in the tunnel is driven by a pump capable of delivering speeds in the range 0.01 m/s - 1 m/s in steps of 0.01 m/s. A set of filters and honeycombs before the test section inlet ensures a steady and uniform flow with very low turbulence levels. Tests to determine exactly how low turbulence levels and other properties of the inflow are planned for 2020. Initial experiments of the boundary layer thickness on the test section walls are performed and estimates that it is in the order of ≅30mm at the middle of the test section at the highest Reynolds numbers. Further detailed investigations are also planned for 2020, however the bump will be designed to be well outside of the boundary layer of the test section and hence only the boundary layer of the splitter-plate will be of importance for the experiments in this test case.

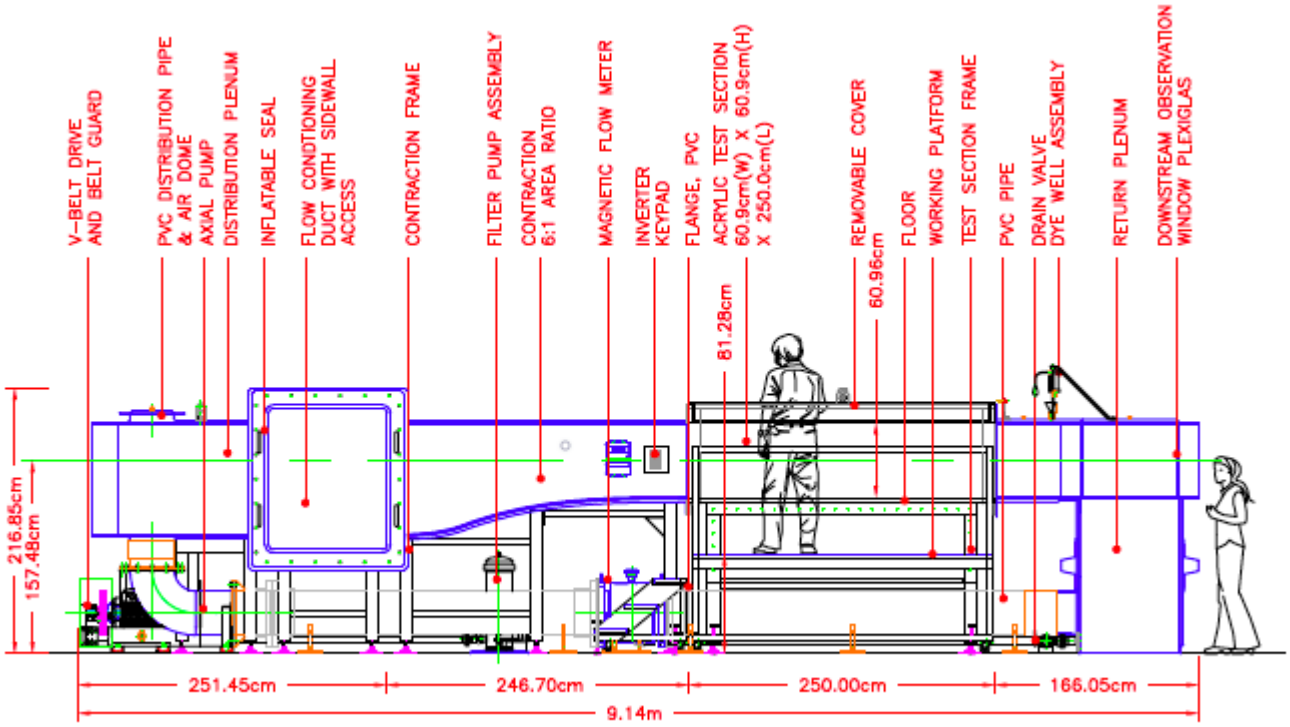

Figure 11: Design sketch of the CWT facility

The tests will be run with a roof to avoid effects of the free surface. Further the bump will be placed on each side of a smooth flat splitter-plate which will be placed horizontally in the middle of the test section. The plate will have a squared leading edge for practical reasons. The mirroring of the bump on both sides of the plate is to ensure that the steady lift on the plate is zero. The plate will be attached to struts going through holes in the roof such that the force sensors are connected to the struts without being underwater. An early concept sketch of the bump mounting in the test section is presented in Figure 12.

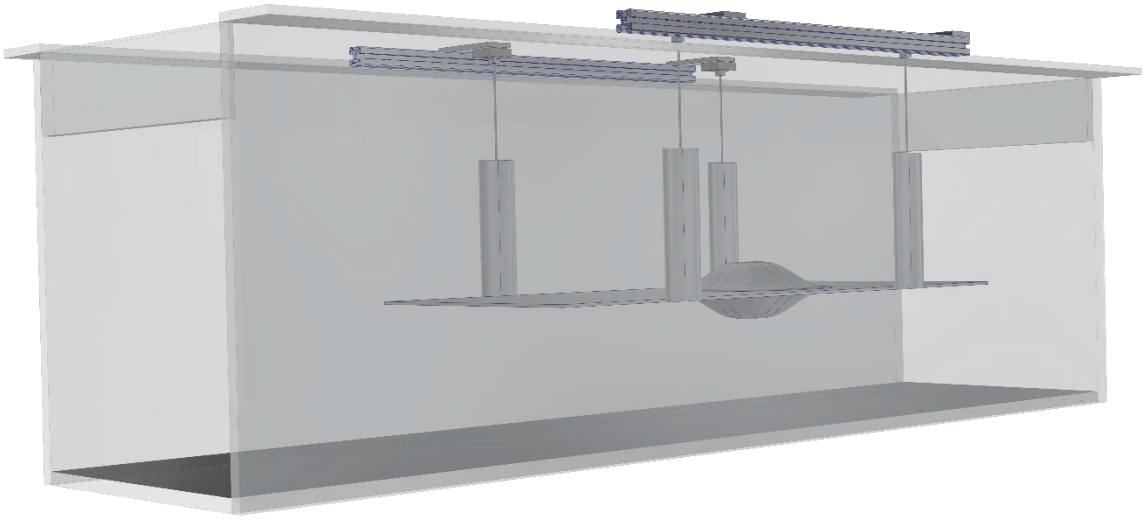

Figure 12: Mounting of the plate and the bumps in the test section

Two setups will be tested. One setup with only the plate and another setup with the bumps mounted on the plate. The reason for this is that the forces on the plate and the struts alone needs to be measured to ensure that they are steady and can be used as zero values. The second setup are an investigation of the boundary layer on the plate without the bumps, both with and without a tripwire. Further the bumps will be able to rotate around their vertical center axis. A set of alignment holes will allow for visually placing both bumps at the desired angles. The alignment holes are 2mm in diameter and will be covered with thin tape to not disturb the flow field. The angles of interest are: 0, 15, 30 and 45 degrees. There will be alignment holes for these angles in the splitter-plate, but there will also be 3 alignment holes on the bump allowing for small adjustments of ±2 degrees relative to the angles of interest such that the sensitivity of the bump's rotation can be investigated. Figure 13 illustrates the screening holes on the bump seen from the top.

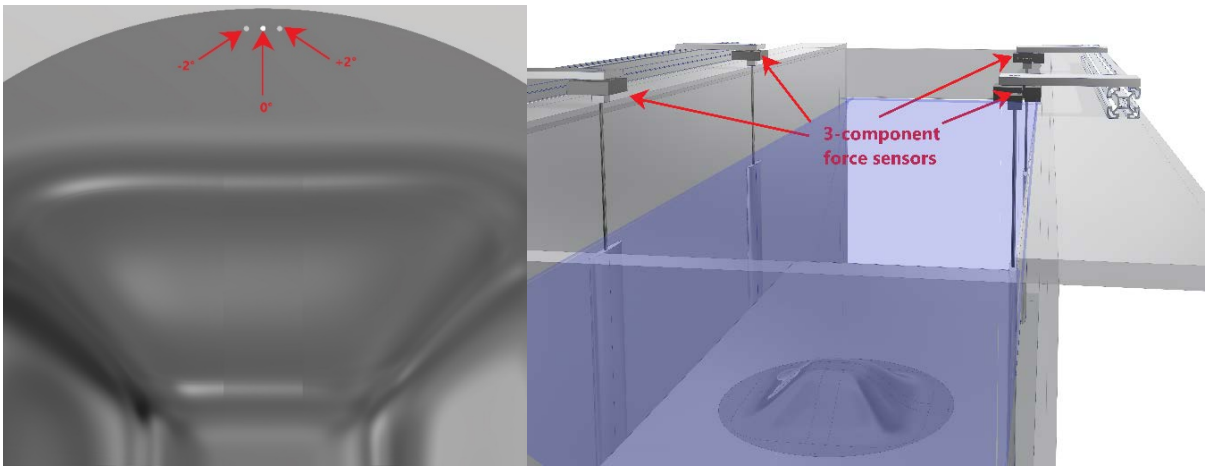

Figure 13: Left: Screening holes in the bump allow for rotations of -2, 0 and +2 degrees relative to the main angles of interest. Right: The force sensors are connected to threaded rods which allows for height adjustments, the rods are threaded into the struts which in turn is connected to the plate.

For the optical measurements both PIV and LDV will be used. A two component MiniLDV-G5L-2D-500 from the company MSE [3] will be used for the LDV experiments. This system has a 785nm and a 658nm laser component measuring 90 degrees to each other. Both components offer frequency shifting such that both positive and negative velocities can be measured. At speeds of 0.9m/s the system is capable of measuring at several hundred hertz, but this is very dependent on the seeding conditions and the type of flow to be measured. The LDV system has a reach of 505mm in air and will be placed at the side of the test section as seen in Figure 14. A traverse system allows for fine adjustment of the measurement location in x-, y- and z-direction.

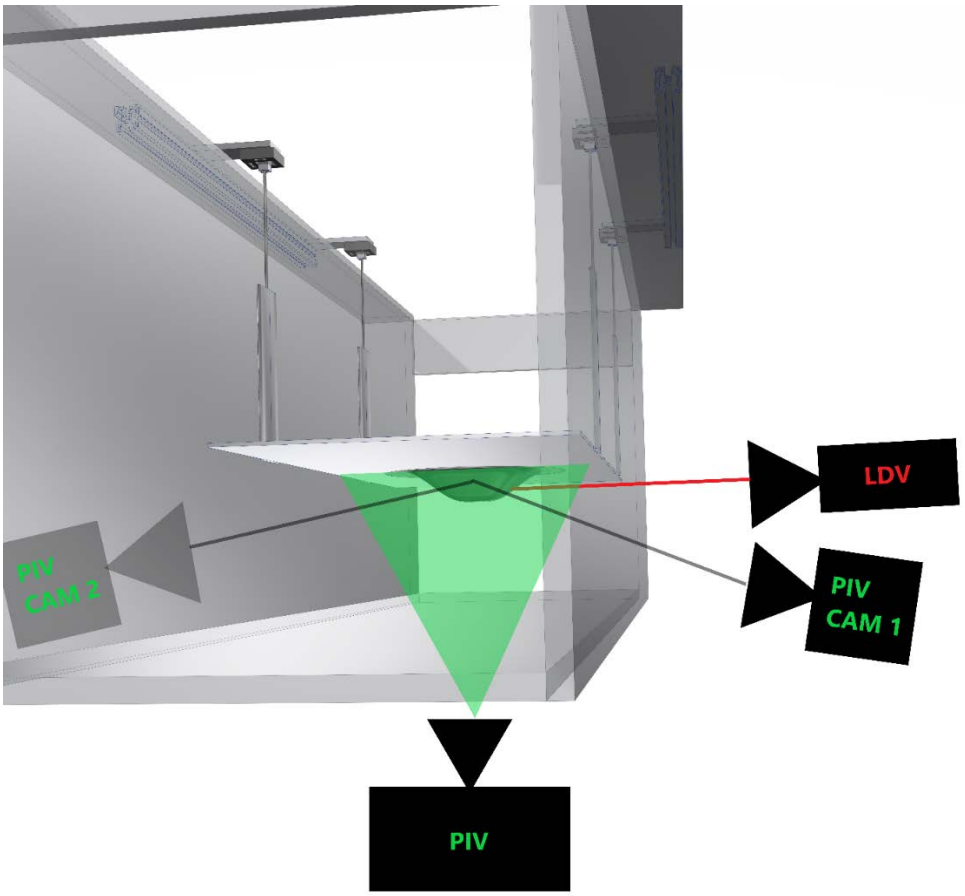

Figure 14: Example of experimental setup of the optical measurements. The LDV laser will shoot in on the bump from the side to measure the boundary layer on the bump, while the PIV laser sheet will come from under the test section. In both cases it is the bottom side bump that will be investigated.

The PIV system comes from the company LaVision [4]. A stereoscopic setup resolving at 15Hz will be used to capture full field velocity components in all three directions. The system uses a 532nm double pulsed Nd:YAG laser that will shoot up from under the test section on the bottom side bump. The PIV cameras can be placed on the same side or on opposite sides of the test section. Additional cameras will be used to triangulate the exact position of the PIV planes.

The test case is supposed to contain key physics of pressure driven, three-dimensional boundary layers with and without separation. The main feature of the flow is a separation bubble on the downstream side of the bump. The experiments should be able to pinpoint the location and extent of this separation bubble including the incipient separation and thickness of the separated area as well as the reattachment position. This is believed to be possible with the aforementioned PIV and LDV system.

However, Gargiulo et al. [2] reports in their sensitivity experiments also a small separation area on the windward side of the bump for smaller Reynolds numbers. The big scale experiments to be done in the Cavitation tunnel are believed to be working at sufficient high Reynolds numbers that this small separation area vanishes, but due to the lower Reynolds number in the CWT, it may be present during these tests. The experiments should therefore aim to observe this high shear area region near the top of the bump

and try to find out how sensitive it is to Reynolds number variations and bump height to boundary layer thickness ratio variations. Even though the incipient separation on the windward side of the bump was clearly visible on the oil flow visualization experiments conducted by Gargiulo et al. they were struggling to capture the separation with PIV concluding that the separation bubble was smaller than 1mm in size. Therefore, flow visualization should be used to map the different flow regimes on the bump that may not be visible with PIV. To do this a fluorescein fluid will be injected at an upstream point of the bump. The flow will then be illuminated with UV-lights for visual observation of separation zones and other flow features of interest.

Overall Test Section Hydrodynamic Conditions

The experiments will be designed for the highest Reynolds number that can be achieved in the CWT facility. Using a safety factor this means that the inflow velocity is 0.9m/s and the Reynolds number based on bump height approximately 54 000 at 20 degrees Celsius. When the water in the tunnel is newly filled it holds a temperature of approximately 5 degrees Celsius, this means that the Reynolds number is only 35 500. This viscosity temperature dependence makes it crucial to know the experimental conditions for every run. To achieve the highest possible Reynolds number the experiments will therefore be run at as high temperatures as possible. Even then the experiments will struggle to obtain a turbulent boundary layer on the plate and a tripwire will have to be used to get the desired flow. Test will also be run for lower Reynolds number all the way down to 1800 to see how this affects the flow.

Previous experiments have found that the turbulence levels in the tunnel is approximately 1% for a free stream velocity at 0.3m/s, but this is believed to be within the noise range of the LDV equipment. Further studies will be conducted to try to get a more reliable measure of the turbulence. Additionally, the inflow uniformity should be studied in more detail to have exact knowledge about what inflow conditions the bump will be subject to. Here previous studies suggest that the mean flow velocity variation $(U_{max} - U_{min})/U_{\infty}$ is somewhere around 2% but as these are only rough estimates based on historical data, additional experiments are needed.

The hydrodynamic properties of the experiments depend in a large degree on the ambient conditions, mainly temperature, at the day of the experiments. More detailed measurements need to be made on the inflow properties of the tunnel to determine exactly what conditions that will be valid for this test case. However typical or estimated conditions are given in the table below.

Design temperature	20°C
Density at design temperature	998.2 kg/m^3
Kinematic viscosity at design temperature	$1.0023 * 10^{-6}\, m^2/s$
Free stream turbulence intensity	<1%

Table 4: Typical hydrodynamic properties

Measurements to be made

a) Water Temperature
b) Turbulence levels of the free flow using LDV for all desired velocities in the test case.
c) Free stream uniformity experiments with PIV at three different cross planes.
    i. Inflow plane
    ii. A plane at the position where the bump will be located
    iii. Outflow plane
d) Plate without bumps
    i. Stability force measurements at all wanted velocities to look for instabilities or oscillation periods in the setup
    ii. Force measurements to capture the zero values.
    iii. Visual experiments with fluorescent dye to check for manufacturing errors and flaws in the design.
    iv. Boundary layer at the plate with PIV and LDV, the main goal is to find the boundary layer thickness at the bump location for all desired speeds both with and without a tripwire. PIV plane 5 and 6 is wanted to check that the edge of the plate does not create any unwanted disturbances at the bump sides.

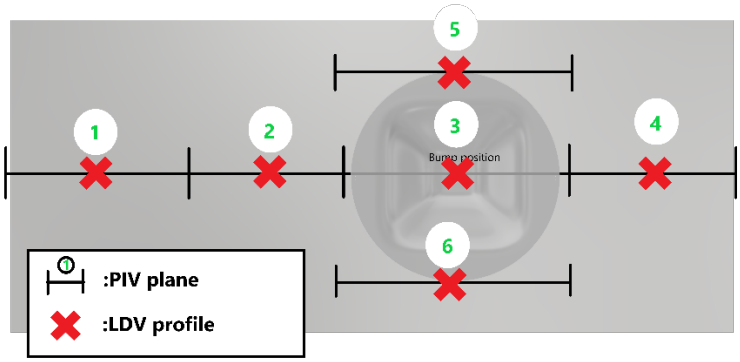

Figure 15: Expected PIV planes and LDV profile locations for boundary layer measurements.

e) Plate with bumps mounted. All the experiments will be run for all the desired angles of the bumps: 0, 15, 30 and 45 degrees. Additional rotations of ±2 degrees relative to this will also be tested for some of the experiments to observe how sensitive the flow regimes are to small rotations.
    i. Stability force measurements
    ii. Force measurements to capture oscillation periods and instabilities.
    iii. Visual experiments with fluorescent dye to map the different flow regimes.
    iv. PIV planes and LDV profiles for velocity fields. Figure 16 illustrates the main categories of the measurement locations. The exact locations and number of planes and profiles will be adjusted as the experiments develops and more knowledge about the flow features and their locations is gathered.
    CV1, SV1 and LDV1: Inflow plane and boundary layer.
    CV2,SV2 and LDV2: Upstream side of bump. Try to locate the small separation area and it's sensitivity to Reynolds number.
    CV3 and SV3: The top side of the bump. Incipient separation

CV4, SV4 and LDV3: Separated area at downstream side of bump.
CV5 and SV5: Downstream reattachment and outflow.

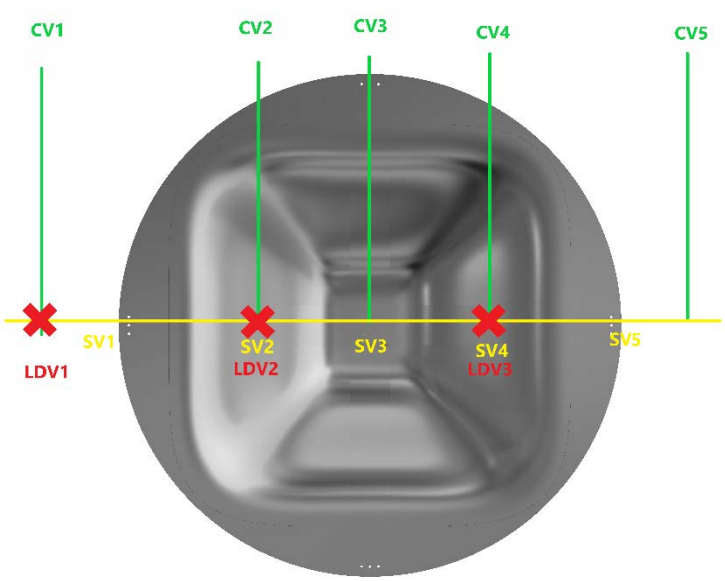

Figure 16: Expected PIV planes and LDV profiles. The figure illustrates the main group of the measurements and not the exact positions.

References

[1] T. Lowe, W. Devenport, J. Duetsch-Patel og A. Garigulo, «Boundary Layer Flow over a Bump: Benchmark Experiments for CFD Validation,» Virginia Tech, 2020.

[2] A. Gargiulo, V. Vishwanathan, D. J. Fritsch, J. E. Duetsch-Patel, M. Szoke, A. Borgoltz, W. J. Devenport, C. J. Roy and K. T. Lowe, "Examination of Flow Sensitivities in Turbulence Model Validation Experiments," in *AIAA SciTech 2020 Forum*, Orlando, FL, Jan 6, 2020., AIAA 2020-1583., 2020.

[3] "Measurements Science Enterprise, inc," 23 March 2020. [Online]. Available: http://measurementsci.com/.

[4] LaVision, "LaVision," [Online]. Available: https://www.lavision.de/en/index.php. [Accessed 23 March 2020].

University of Toronto Institute for Aerospace Studies Experiment

Complementary experiments will be performed at the University of Toronto Institute for Aerospace Studies (UTIAS). For these experiments, a scaled model of the bump will be tested in the low-speed wind tunnel at UTIAS. The tunnel can operate up to 35 m/s with a freestream turbulence intensity of roughly 0.05% up to 13 m/s, monotonically growing to 0.08% at full speed. The 5-m long working section has an octagonal cross-section that is 0.8 m high and 1.2 m wide. The corners of the test-section are nominally 0.28 m wide and are adjustable such that a near-zero pressure gradient can be achieved along the test-section length.

The width and height of the bump model for the experiments at UTIAS will be 0.6 m and 0.12 m, respectively. The model will be mounted on a flat-plate that will be used to grow a new turbulent boundary layer, similar to the setup from Belanger et al. (2019) [1]. The plate spans the full 1.2 m width of the working section and is approximately 5 m long, with a 0.4 m flap at the tailing edge to control the location of the stagnation line at its asymmetric leading edge. A zig-zag trip is applied near the leading edge to force early, spanwise uniform transition to turbulence, see Figure 17. The plate will be mounted 0.23 m above the test section floor, which is between ¼ and 1/3 of the test-section height to minimize potential effects from secondary flows. The model leading edge will be located at approximately 2.5 m from the leading edge of the plate.

At the maximum speed of the tunnel, the nominal test conditions are

$$
\begin{aligned}
U &= 35\ \mathrm{m/s} \\
Re_\theta &= 9\mathrm{k} \\
Re_h &= 280\mathrm{k} \\
M_\infty &= 0.10 \\
h/\theta &= 30 \\
h/\delta &= 2.9 \\
w_{bump}/w_{tunnel} &= 0.5
\end{aligned}
$$

An example of the inflow boundary layer profile for a case at a greater Reynolds number ($Re_\theta = 17k$) is shown in Figure 17.

Figure 17. Photo of boundary layer plate inside the wind tunnel at UTIAS looking towards the downstream end of the working section.

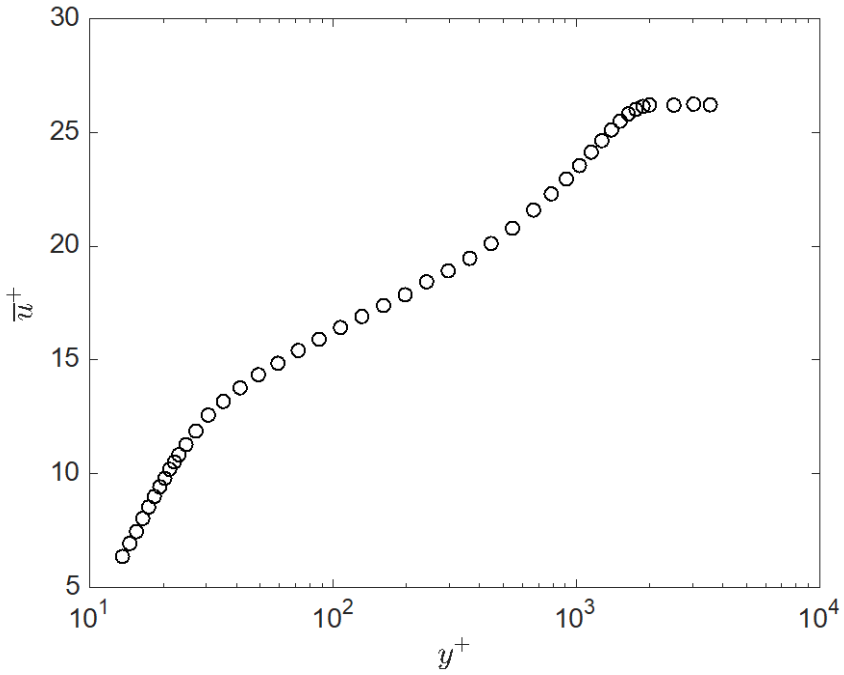

Figure 18. Velocity profile of the turbulent boundary layer for $Re_\theta = 17k$.

References

[1] Belanger R.K.R., Zingg DW, Lavoie P (2019) Synthetic jet forcing of large-scale fluctuations in a turbulent boundary layer. In Proc. 11th International Symposium on Turbulence and Shear Flow Phenomena (TSFP11), Southampton, UK, July 30 to August 2, 2019.